Biophysical Chemistry 143 (2009) 166–169

Contents lists available at ScienceDirect

Biophysical Chemistry

journal homepage: http://www.elsevier.com/locate/biophyschem

Short communication

Studies of a viral suppressor of RNA silencing p19-CFP fusion protein: A FRET-based probe for sensing double-stranded fluorophore tagged small RNAs

Roger Koukiekolo [a], Zygmunt J. Jakubek [a], Jenny Cheng [a], Selena M. Sagan [a,b], John Paul Pezacki [a,b,*]

[a] Steacie Institute for Molecular Sciences, National Research Council of Canada, 100 Sussex Drive, Ottawa, Canada K1A 0R6
[b] Department of Biochemistry, Microbiology and Immunology and the Ottawa Institute of Systems Biology, University of Ottawa, Ottawa, Canada K1H 8M5

ARTICLE INFO

Article history:
Received 16 April 2009
Received in revised form 6 May 2009
Accepted 6 May 2009
Available online 12 May 2009

Keywords:
RNA silencing
Carnation Italian ringspot virus
Chemical probes
RNA–protein interactions
FRET

ABSTRACT

Eukaryotes have evolved complex cellular responses to double-stranded RNA. One response that is highly conserved across many species is the RNA silencing pathway. Tombusviruses have evolved a mechanism to evade the RNA silencing pathway that involves a small protein, p19, that acts as a suppressor of RNA silencing. This protein binds specifically to small-interfering RNAs (siRNAs) with nanomolar affinity in a sequence-independent manner and with size selectivity.

1. Introduction

The *Aequorea victoria* green fluorescent protein (GFP) has been widely applied for imaging and as both donor and acceptor molecules for Förster resonance energy transfer (FRET) to report on the distance-dependent molecular interactions and for the biosensing of molecular binding events *in vitro* and *in vivo* [1–4]. For example, engineered 'chameleon' proteins that include the fusion of the donor cyan fluorescent protein (CFP), a calmodulin domain, the calmodulin binding domain of myosin light chain kinase, and an acceptor yellow fluorescent protein (YFP) have been very successful at sensing calcium concentration gradients in living systems using FRET [4–7]. Genetically encoded FRET-based probes have also been successfully applied to the examination of receptor function, protein dimerization and a host of other physiologically relevant biomolecular interactions [3,4,8–12]. Yet few examples exist where such fusion proteins have been applied to sense RNA. FRET-based approaches have been applied to sense RNA. For example, molecular beacons have been used successfully to sense oligonucleotides [13–19]; however, the application of these probes to visualize RNA with size- and sequence-specificity remains challenging. Here we demonstrate a simple fusion protein based on the Carnation Italian ringspot virus protein p19 [20–27] and CFP. The p19 protein is able to suppress RNA silencing by binding and sequestering 21 nucleotide (nt) short interfering RNAs (siRNAs). The p19-CFP fusion protein reported herein can sense small RNAs through intermolecular FRET from CFP donor to the Cy3 acceptor attached to siRNA (Scheme 1).

The cellular double-stranded RNA (dsRNA) response is a critical component of the cellular response to RNA viruses in eukaryotes [28], and the evolutionarily conserved RNA silencing pathway represents an important part [29–34]. Tombusviruses, a family of single-stranded RNA viruses of plants, have adapted a mechanism to evade RNA silencing that involves a 19 kDa protein (p19) that acts as an siRNA inhibitor [21–23,35]. Dimeric p19 binds to and sequesters siRNAs preventing their incorporation into the RISC [21–23,35]. The p19 dimer also binds selectively to 21-nt double-stranded siRNA with high affinity in a size-selective and relatively sequence-independent manner. A number of assays for siRNA detection and quantification have been developed based on p19 because of its ability to act as a molecular ruler and distinguish between different types of small RNAs [24–27,36,37]. Here we establish the use of a Carnation Italian ringspot virus (CIRV) p19-CFP fusion protein and Cy3 labeled siRNA as a suitable FRET pair for the convenient and rapid sensing of siRNA protein interactions. Described herein are the steady-state fluorescence studies of the FRET pair that demonstrate its utility as a probe for small RNA sensing.

2. Experimental methods

2.1. Cloning of CIRV 2x-p19-CFP

The pTriEx-2x-p19-CFP recombinant plasmid was designed from the linked dimer vector, CIRV p19-2x-p19-H, constructed previously [24].

* Corresponding author. Steacie Institute for Molecular Sciences, National Research Council of Canada, 100 Sussex Drive, Ottawa, Canada K1A 0R6. Tel.: +1 613 993 7253; fax: +1 613 941 8447.
E-mail addresses: Roger.Koukiekolo@nrc.ca (R. Koukiekolo), Zygmunt.Jakubek@nrc.ca (Z.J. Jakubek), Jenny.Cheng@nrc.ca (J. Cheng), Selena.Sagan@nrc.ca (S.M. Sagan), John.Pezacki@nrc-cnrc.gc.ca (J.P. Pezacki).

0301-4622/$ – see front matter © 2009 Elsevier B.V. All rights reserved.
doi:10.1016/j.bpc.2009.05.001

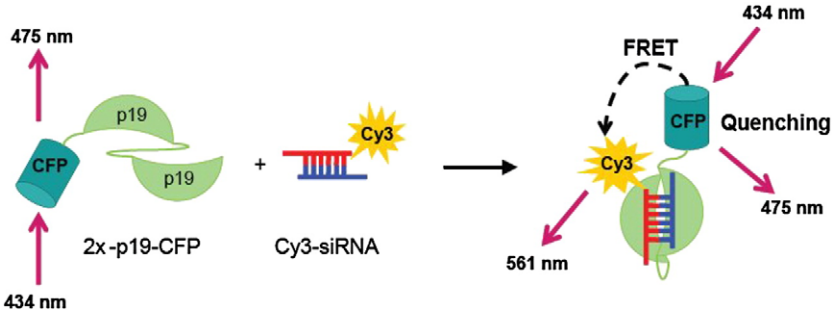

Scheme 1. FRET detection developed using the 2x-p19-CFP protein. Excitation of CFP at 434 nm leads to FRET to the acceptor Cy3 attached to CSK siRNA detected at 561 nm.

The BamHI restriction site was generated at the N-terminus of p19-2x-p19 sequence using the site-directed mutagenesis resulting to the construct pTriEx-BamHI-p19-2x-p19. Mutagenesis reactions were carried out employing the QuickChange II site-directed mutagenesis kit (Stratagene) and a pair of complementary mutagenic primers. The sequence of the forward primer was designed as follow: sense 5′-AGATATACCATGGAAGGATCCCGCGCTATC-3′ and anti-sense 5′-GATAGCGCGGGATCCTTCCATGGTATATCT-3′. The integrity of the mutated plasmid was confirmed by sequencing. The DNA plasmid template pOpsin-CFP was kindly provided by Paul Shin-Hyun Park (Department of Pharmacology, Case Western Reserve University, Cleveland). pOpsin-CFP encodes an enhanced cyan fluorescent variant of the *Aequorea victoria* green fluorescent protein gene (GFP). The coding region of CFP gene was amplified from pOpsin-CFP by PCR using gene-specific primer sets that are flanked by BamHI (sense 5′-CGAGGATCCATGGTGAGCAAGGGC-3′ and anti-sense 5′-AGTCGCGGCCGGATCCCTTGTACAGCTCGTCCATGC). The amplified BamHI PCR product was digested with BamHI and inserted into BamHI-cleaved pTriEx-BamHI-p19-2x-p19. The resultant construct, pTriEx-2x-p19-CFP, was confirmed by sequencing.

2.2. Protein expression and purification

Bacterial overexpression of CIRV 2x-p19-CFP was carried out in *Escherichia coli* strain BL21 (DE3) cells harboring the pTriEX-2x-p19-CFP construct at 37 °C until an OD_{600} of 0.5–0.6 was achieved. Expression of CIRV 2x-p19-CFP was induced by IPTG at a final concentration of 1 mM. Cultures were then grown for an additional 4–5 h at 30 °C. Bacterial pellets were resuspended in lysis buffer (50 mM NaH_2PO_4, 300 mM NaCl, 10 mM imidazole, 1 mM DTT (pH 8.0) and lysed by sonication on ice. The CIRV 2x-p19-CFP protein was purified from the soluble fraction of lysate by binding to a Ni^{2+}-NTA column (Pharmacia, Peapack, NJ). The resin was washed with wash buffer (50 mM NaH_2PO_4, 500 mM NaCl, 20 mM imidazole, 1% Tween 20, pH 8. Elution of CIRV 2x-p19-CFP was carried out with elution buffer (50 mM NaH_2PO_4, 300 mM NaCl, 250 mM imidazole, pH 8.0). The pooled eluates were desalted using the PD-10 column (Pharmacia, Peapack, NJ) and concentrated into 1 ml of 50 mM Tris–HCl, 150 mM NaCl buffer (pH 8.0) using the Ultrafree 10-kDa membrane (Millipore, Concord, MA). The protein purity for samples used for FRET studies was determined to be more than 95% by SDS-PAGE and analytical gel filtration experiments.

2.3. Fluorescence resonanance energy transfer measurements

Steady state fluorescence measurements were carried out using a Fluorolog Tau-3 spectrofluorometer (Horiba Jobin Yvon, Edison, NJ). All measurements were carried out using a 10 mm quartz cell. Sample solution containing 100 nM 2x-p19-CFP was incubated at room temperature in a solution containing phosphate buffered saline (50 mM potassium phosphate, pH 7.2; 150 mM NaCl) and aliquots of Cy3-siRNA were added to the desired concentration varying from 0 to 2 μM. After a 30 min-long equilibration following each addition, fluorescence emission spectra were recorded. The sample was excited at 434 nm with 2 nm excitation light band width and fluorescence spectra were recorded in the 450–700 nm range. Fluorescence intensities were measured at 475 nm and 561 nm, i.e. at maximum intensity of 2x-p19-CFP and Cy3-siRNA fluorescence bands, respectively. Quenching or fluorescence enhancement effects were evaluated using plots of corrected fluorescence intensity (integrated emission spectrum) versus concentration of Cy3-siRNA. Data was analyzed using Origin™ 7.0 graphing analysis software (Northampton, MA).

3. Results and discussion

3.1. Cloning of 2x-p19-CFP

Our primary goal in this work was to generate a genetically encoded fusion protein containing the p19 dimer and the FRET donor (CFP) that retained its ability to bind with size selectivity to small RNAs and to demonstrate its ability to undergo FRET with dye tagged RNAs. Previously we reported linking the C-terminus of one p19 to the N-terminus of a second p19 monomer with $(GGGGS)_2$ linker sequences (2x-p19) and that this linked dimer had 3-fold higher affinity compared to wild-type p19 and retained size selectivity for 21-nt siRNAs [24]. Functional GFP-fusion proteins of p19 have also been reported recently [38,39]. Here we incorporated CFP analogously [38,39] into the recombinant 2x-p19 to yield a 2x-p19-CFP. This represents a genetically encoded single molecule containing the p19 dimer and the FRET donor (CFP).

3.2. FRET measurements between 2x-p19-CFP and Cy3-labeled siRNA

We have studied the interaction of 2x-p19-CFP with a Cy3-labeled double-stranded siRNA (Cy3-siRNA) that targets the human kinase CSK in buffered solutions. Our goal was to evaluate suitability of the 2x-p19-CFP for measuring protein-RNA interactions in FRET-based assays. We performed several experiments starting with 100 nM 2x-p19-CFP and varying the concentration of Cy3-siRNA. Control experiments were also performed using 2x-p19-CFP with unlabeled siRNA, 2x-p19-CFP with Cy3 dye only, 2x-p19 (unlabeled) with Cy3, and 2x-p19 with Cy3-siRNA. We only observed concentration-dependent FRET between 2x-p19-CFP and Cy3-siRNA (Fig. 1).

Significant suppression of the CFP fluorescence at 475 nm was observed with varying concentration of Cy3-siRNA (Fig. 1). Although we did observe significant Cy3 fluorescence at 561 nm, some of it appeared not to originate from CFP→Cy3 FRET. To determine the Cy3 fluorescence arising only from FRET, the fluorescence signal was corrected for the cross-channel effects, i.e. CFP donor fluorescence at 561 nm and Cy3 acceptor fluorescence directly excited at 434 nm (i.e. donor excitation wavelength), and buffer background signal.

3.3. Binding measurement of 2x-p19-CFP fluorescence by Cy3-labeled siRNA

The CFP fluorescence is clearly efficiently quenched allowing for binding interactions to be determined and affinity measurements to

be made (Fig. 2). The 2x-p19-CFP fluorescence quenching due to binding of the Cy3-siRNA to the recombinant protein experiments were conducted by exciting 2x-p19-CFP donor and measuring unquenched CFP fluorescence intensity while varying the acceptor Cy3-siRNA concentration. The 2x-p19-CFP concentration was 100 nM. The resulting concentration-dependent increase in FRET as measured by the CFP donor fluorescence intensity, F, as a function of Cy3-labeled siRNA concentration, x, was fit by least-squares nonlinear regression to the binding model given by the following equation as previously reported [27]:

$$\Delta F = \Delta F_{\mathrm{Max}}\left(\frac{K_{\mathrm{d}} + np + x}{2np} - \sqrt{\left(\frac{K_{\mathrm{d}} + np + x}{2np}\right)^2 - \frac{x}{np}}\right) \quad (1)$$

where ΔF_{Max} denotes the maximal change in fluorescence intensity of CFP, K_{d} is the dissociation constant, n is the number of equivalent sites on the p19 dimer, p is the concentration of labeled small RNA, x is the concentration of the p19 dimer.

In these experiments a concentration of 100 nM 2x-p19-CFP was used (Fig. 2) and the concentration of Cy3-siRNA was varied in the 0–2 μM range. The measured dissociation constant was determined to be $K'_{\mathrm{d}} = 22 \pm 5.2$ nM. The K'_{d} value agrees very well with the values of 15 ± 7 and 21 ± 3 nM measured by fluorescence polarization and electrophoretic mobility shift assay methods, respectively, for the p19 under similar conditions [27]. This suggests that the CFP fusion has a negligible effect on p19′s ability to bind to its target siRNA. The magnitude of the binding constant is consistent with the high affinity of 2x-p19-CFP for duplex 21-nt RNA. It also demonstrates the potential for FRET probes based on p19 to efficiently report on small RNAs.

We do observe that there is a fraction of unquenchable CFP. There are two possible sources for the unquenchable signal. Firstly, it may be possible that alternative binding modes for Cy3-labeled CSK siRNA exist. There are at least two possible siRNA orientations within the binding pocket of p19 and one of these may result in inefficient CFP quenching. Using the known structure of p19 we estimate that two alternative binding orientations may result in a 4- to 6-fold change in the CFP-Cy3 distance. This would result in quenching efficiency varying by approximately 4 orders of magnitude between these two binding modes. Secondly, it is well known that p19 sometimes forms aggregates at higher concentrations and in an oxidizing environment [24–27,36,37]. It is possible that a dimer or an oligomer of 2x-p19-CFP is giving rise to a component that is unquenchable. To confirm this hypothesis we performed size exclusion chromatography. At 2 μM concentration of 2x-p19-CFP we do observe peaks corresponding to the expected monomeric form 2x-p19-CFP as well as peaks consistent with the expected molecular weights of 2x-p19-CFP dimers and tetramers. However, the monomeric 2x-p19-CFP is still the major component (greater than 50%). At 100 nM concentration of 2x-p19-CFP the monomeric fraction is expected to be significantly larger.

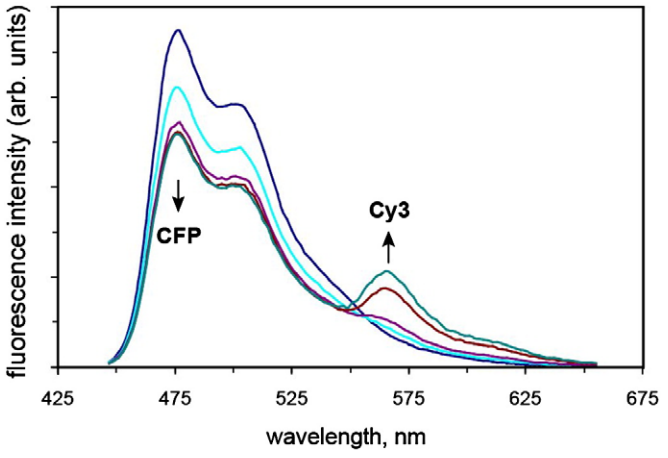

Fig. 1. Fluorescence spectra of 2x-p19-CFP fusion protein (100 nM) and Cy3 labeled RNA in solution. Emission spectra of 2x-p19-CFP were acquired at an excitation wavelength of 434 nm for zero and varying concentrations of Cy3-siRNA (0, 5, 10, 100, and 200 nM). Each spectrum was corrected for cross-channel effects by subtracting the spectra of unlabeled 2x-p19 and Cy3-siRNA acquired at the corresponding concentrations.

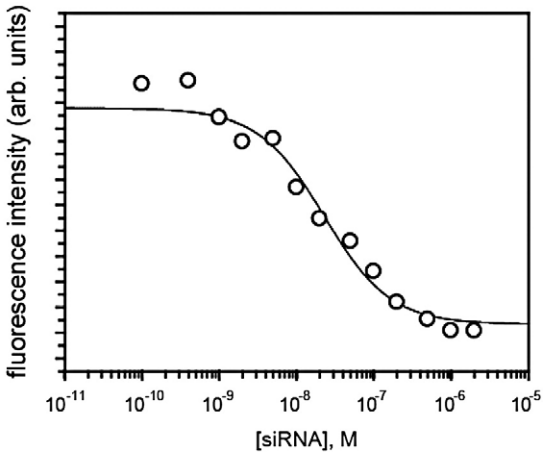

Fig. 2. Binding plot for 2x-p19-CFP with Cy3-siRNA as measured by FRET using 100 nM 2x-p19-CFP and the concentration of CSK Cy3-siRNA varying in the 0–2 μM range at pH 7.4 in 50 mM phosphate buffer at 21 °C, as previously described for other p19 variants.

We found that 2x-p19-CFP also did show size selectivity and did not bind appreciably to either single-stranded RNA or to a 28-nt siRNA targeting the luciferase gene [26]. CFP does not appear to cause steric hindrance to the binding of the siRNA to the p19 dimer or limit its ability to adopt an ideal conformation for siRNA binding. We observe a size-selective interaction of 2x-p19-CFP with ds 21-nt siRNAs making 2x-p19-CFP a good probe for small duplex RNAs.

4. Conclusions

In summary, we have described a fusion protein based on the siRNA suppressor protein p19 that is fused to CFP. This fusion protein can undergo FRET with dye labeled siRNA and this allows for the direct sensing of the protein-RNA interaction in solution. The 2x-p19-CFP maintains its ability to act as a molecular ruler by binding duplex siRNAs in a size-selective manner. It can distinguish between double-stranded small RNAs and their single-stranded counterparts that may arise from melting or have been unwound by components of the RISC complex. This represents a novel strategy for siRNA sensing, and a starting point for the development of other such tools that may report on siRNAs without the necessity for labeling of the siRNA *in vivo*.

References

[1] R.Y. Tsien, A. Miyawaki, Seeing the machinery of live cells, Science 280 (1998) 1954–1955.
[2] B.A. Pollok, R. Heim, Using GFP in FRET-based applications, Trends Cell Biol. 9 (1999) 57–60.
[3] J. Zhang, R.E. Campbell, A.Y. Ting, R.Y. Tsien, Creating new fluorescent probes for cell biology, Nat. Rev., Mol. Cell Biol. 3 (2002) 906–918.
[4] A. Miyawaki, Visualization of the spatial and temporal dynamics of intracellular signaling, Dev. Cell 4 (2003) 295–305.
[5] A. Miyawaki, J. Llopis, R. Heim, J.M. McCaffery, J.A. Adams, M. Ikura, R.Y. Tsien, Fluorescent indicators for Ca2+ based on green fluorescent proteins and calmodulin, Nature 388 (1997) 882–887.
[6] T. Nagai, A. Sawano, E.S. Park, A. Miyawaki, Circularly permuted green fluorescent proteins engineered to sense Ca2+, Proc. Natl. Acad. Sci. U. S. A. 98 (2001) 3197–3202.
[7] K. Truong, A. Sawano, H. Mizuno, H. Hama, K.I. Tong, T.K. Mal, A. Miyawaki, M. Ikura, FRET-based in vivo Ca2+ imaging by a new calmodulin–GFP fusion molecule, Nat. Struct. Biol. 8 (2001) 1069–1073.

[8] A. Terskikh, A. Fradkov, G. Ermakova, A. Zaraisky, P. Tan, A.V. Kajava, X.N. Zhao, S. Lukyanov, M. Matz, S. Kim, I. Weissman, P. Siebert, "Fluorescent timer": protein that changes color with time, Science 290 (2000) 1585–1588.
[9] N. Mochizuki, S. Yamashita, K. Kurokawa, Y. Ohba, T. Nagai, A. Miyawaki, M. Matsuda, Spatio-temporal images of growth-factor-induced activation of Ras and Rap1, Nature 411 (2001) 1065–1068.
[10] R. Ando, H. Mizuno, A. Miyawaki, Regulated fast nucleocytoplasmic shuttling observed by reversible protein highlighting, Science 306 (2004) 1370–1373.
[11] A. Muller-Taubenberger, K.I. Anderson, Recent advances using green and red fluorescent protein variants, Appl. Microbiol. Biotechnol. 77 (2007) 1–12.
[12] M. Kitano, M. Nakaya, T. Nakamura, S. Nagata, M. Matsuda, Imaging of Rab5 activity identifies essential regulators for phagosome maturation, Nature 453 (2008) 241-215.
[13] W.H. Tan, K.M. Wang, T.J. Drake, Molecular beacons, Curr. Opin. Chem. Biol. 8 (2004) 547–553.
[14] V.V. Lunyak, R. Burgess, G.G. Prefontaine, C. Nelson, S.H. Sze, J. Chenoweth, P. Schwartz, P.A. Pevzner, C. Glass, G. Mandel, M.G. Rosenfeld, Corepressor-dependent silencing of chromosomal regions encoding neuronal genes, Science 298 (2002) 1747–1752.
[15] B. Dubertret, M. Calame, A.J. Libchaber, Single-mismatch detection using gold-quenched fluorescent oligonucleotides, Nat. Biotechnol. 19 (2001) 365–370.
[16] N. Hamaguchi, A. Ellington, M. Stanton, Aptamer beacons for the direct detection of proteins, Anal. Biochem. 294 (2001) 126–131.
[17] G. Bonnet, S. Tyagi, A. Libchaber, F.R. Kramer, Thermodynamic basis of the enhanced specificity of structured DNA probes, Proc. Natl. Acad. Sci. U. S. A. 96 (1999) 6171–6176.
[18] A.S. Piatek, S. Tyagi, A.C. Pol, A. Telenti, L.P. Miller, F.R. Kramer, D. Alland, Molecular beacon sequence analysis for detecting drug resistance in Mycobacterium tuberculosis, Nat. Biotechnol. 16 (1998) 359–363.
[19] D.L. Sokol, X.L. Zhang, P.Z. Lu, A.M. Gewitz, Real time detection of DNA RNA hybridization in living cells, Proc. Natl. Acad. Sci. U. S. A. 95 (1998) 11,538–11,543.
[20] M. Turina, R. Omarov, J.F. Murphy, C. Bazaldua-Hernandez, B. Desvoyes, H.B. Scholthof, A newly identified role for Tomato bushy stunt virus P19 in short distance spread, Mol. Plant Pathol. 4 (2003) 67–72.
[21] J.M. Vargason, G. Szittya, J. Burgyan, T.M.T. Hall, Size selective recognition of siRNA by an RNA silencing suppressor, Cell 115 (2003) 799–811.
[22] R. Omarov, K. Sparks, L. Smith, J. Zindovic, H.B. Scholthof, Biological relevance of a stable biochemical interaction between the tombusvirus-encoded P19 and short interfering RNAs, J. Virol. 80 (2006) 3000–3008.
[23] H.B. Scholthof, Timeline — the Tombusvirus-encoded P19: from irrelevance to elegance, Nat. Rev. Microbiol. 4 (2006) 405–411.
[24] J. Cheng, S.M. Sagan, N. Assem, R. Koukiekolo, N.K. Goto, J.P. Pezacki, Stabilized recombinant suppressors of RNA silencing: functional effects of linking monomers of Carnation Italian Ringspot virus p19, Biochim. Biophys. Acta-Proteins and Proteomics 1774 (2007) 1528–1535.
[25] R. Koukiekolo, S.M. Sagan, J.P. Pezacki, Effects of pH and salt concentration on the siRNA binding activity of the RNA silencing suppressor protein p19, FEBS Lett. 581 (2007) 3051–3056.
[26] S.M. Sagan, R. Koukiekolo, E. Rodgers, N.K. Goto, J.P. Pezacki, Inhibition of siRNA binding to a p19 viral suppressor of RNA silencing by cysteine alkylation, Angew. Chem., Int. Ed. 46 (2007) 2005–2009.
[27] J. Cheng, S.M. Sagan, Z.J. Jakubek, J.P. Pezacki, Studies of the interaction of the viral suppressor of RNA silencing protein p19 with small RNAs using fluorescence polarization, Biochemistry 47 (2008) 8130–8138.
[28] G.J. Hannon, RNA interference, Nature 418 (2002) 244–251.
[29] E. Bernstein, A.A. Caudy, S.M. Hammond, G.J. Hannon, Role for a bidentate ribonuclease in the initiation step of RNA interference, Nature 409 (2001) 363–366.
[30] S.M. Elbashir, J. Harborth, W. Lendeckel, A. Yalcin, K. Weber, T. Tuschl, Duplexes of 21-nucleotide RNAs mediate RNA interference in cultured mammalian cells, Nature 411 (2001) 494–498.
[31] S.M. Elbashir, W. Lendeckel, T. Tuschl, RNA interference is mediated by 21- and 22-nucleotide RNAs, Genes Dev. 15 (2001) 188–200.
[32] A. Fire, S.Q. Xu, M.K. Montgomery, S.A. Kostas, S.E. Driver, C.C. Mello, Potent and specific genetic interference by double-stranded RNA in *Caenorhabditis elegans*, Nature 391 (1998) 806–811.
[33] S.M. Hammond, S. Boettcher, A.A. Caudy, R. Kobayashi, G.J. Hannon, Argonaute2, a link between genetic and biochemical analyses of RNAi, Science 293 (2001) 1146–1150.
[34] P.D. Zamore, T. Tuschl, P.A. Sharp, D.P. Bartel, RNAi: double-stranded RNA directs the ATP-dependent cleavage of mRNA at 21 to 23 nucleotide intervals, Cell 101 (2000) 25–33.
[35] W.P. Qiu, J.W. Park, H.B. Scholthof, Tombusvirus p19-mediated suppression of virus-induced gene silencing is controlled by genetic and dosage features that influence pathogenicity, Mol. Plant-Microb. Interact. 15 (2002) 269–280.
[36] H. Vogler, R. Akbergenov, P.V. Shivaprasad, V. Dang, M. Fasler, M.O. Kwon, S. Zhanybekova, T. Hohn, M. Heinlein, Modification of small RNAs associated with suppression of RNA silencing by tobamovirus replicase protein, J. Virol. 81 (2007) 10,379–10,388.
[37] J.M. Calabrese, P.A. Sharp, Characterization of the short RNAs bound by the P19 suppressor of RNA silencing in mouse embryonic stem cells, RNA 12 (2006) 2092–2102.
[38] T. Canto, J.F. Uhrig, M. Swanson, K.M. Wright, S.A. MacFarlane, Translocation of Tomato bushy stunt virus P19 protein into the nucleus by ALY proteins compromises its silencing suppressor activity, J. Virol. 80 (2006) 9064–9072.
[39] J.F. Uhrig, T. Canto, D. Marshall, S.A. MacFarlane, Relocalization of nuclear ALY proteins to the cytoplasm by the tomato bushy stunt virus P19 pathogenicity protein, Plant Physiol. 135 (2004) 2411–2423.